ELSEVIER

Thermochimica Acta 318 (1998) 239–244

thermochimica acta

Crystallization of amorphous calcium carbonate

Nobuyoshi Koga*, Yuzou Nakagoe, Haruhiko Tanaka

Chemistry Laboratory, Faculty of School Education, Hiroshima University, 1-1-1 Kagamiyama, Higashi-Hiroshima 739-8524, Japan

Received 12 September 1997; accepted 2 February 1998

Abstract

Amorphous precipitates of $CaCO_3$ were prepared by reacting a mixed solution of Na_2CO_3–NaOH with a $CaCl_2$ solution at various pH ($\geq$11.2) at an ambient temperature of 278 K. The precipitates prepared at pH ranging from 11.2 to 13.0 were identified as amorphous calcium carbonate (ACC) by means of TG–DTA, FT-IR spectroscopy and powder X-ray diffractometry. This showed loss of absorbed water until ca. 530 K and subsequent crystallization to calcite. The crystallization temperature of ACC varied depending on the pH value of sample preparation. The crystallization processes of ACC prepared at various pH values were investigated by DSC. The enthalpy change and activation energy of the crystallization process increased with increasing pH value of sample preparation, ranging from 3.99 to 12.26 kJ (mol $CaCO_3$)$^{-1}$ and from 151.6 to 304.1 kJ mol^{-1}, respectively. The morphologies of ACC and its crystallization product were observed by scanning electron microscopy. It was shown that finely dispersed particles of crystalline calcium carbonate can be prepared through the crystallization of ACC by heating up to ca. 630 K. © 1998 Elsevier Science B.V.

Keywords: Amorphous; Calcium carbonate; Crystallization; Enthalpy change; Kinetics

1. Introduction

Preparation of amorphous calcium carbonate (ACC) in an aqueous medium has been widely reported [1]. Although ACC is unstable in an atmospheric condition of high water vapor pressure, it is promising to use ACC as a precursor of the ceramic processing including calcium oxide, due to the higher reactivity compared with crystalline calcium carbonate. It is known that, when heating ACC, the mass-loss due to the thermal dehydration of absorbed water is first observed, followed by the crystallization to calcite. Recently, it was reported by Kojima et al. [2] that the crystallization temperature of ACC prepared from an aqueous $CaCl_2$–Na_2CO_3–NaOH system changes drastically depending on pH of the aqueous system. It is expected from the change in the crystallization temperature that the amorphous state of ACC changes depending on the pH of preparation. Thermodynamic and kinetic approaches to the crystallization process of ACC are useful to reveal the change in ACC and their influence on the kinetics of the crystallization process. The different crystallization processes expected for ACC prepared at different pH may also influence the morphology and particle size of the crystallization product. A systematic investigation on the crystallization of ACC seems to provide some fundamental knowledge useful in utilizing the ACC of a single phase or in a co-precipitated precursor for many systems of ceramic processing.

*Corresponding author.

PII S0040-6031(98)00348-7

In the present study, a series of ACCs are prepared from an aqueous system of $CaCl_2$–Na_2CO_3–NaOH at various pH, in accordance with Kojima et al. [2]. The dependence of the thermal behavior and crystallization temperature of ACC on the pH of the mother aqueous system is reexamined in order to confirm the reproducibility of the thermal properties of ACC. The enthalpy change and the kinetics of the crystallization of ACC are investigated by DSC. The influence of pH of the mother aqueous system on the thermodynamic and kinetic characteristics of the crystallization process, together with the consequent variations of the morphology and particle size of the crystallization products, is discussed.

2. Experimental

2.1. Sample preparation

Equivolumes of aqueous solutions of sodium carbonate (0.1 mol dm^{-3}) and sodium hydroxide (0–2.0 mol dm^{-3}) were mixed with mechanical stirring, to obtain mixed solutions with various pH. The mixed solutions and an aqueous solution of calcium chloride (0.1 mol dm^{-3}) were kept in a refrigerator at 278 K for 1 h. Equimolar calcium chloride solution with respect to carbonate ions in the mixed solutions was added rapidly to the mixed solutions with mechanical stirring at an ambient temperature of 278 K. The precipitated colloidal phase was filtered immediately and washed with acetone. The precipitates were dried in a vacuum desiccator for one day.

2.2. Measurements

Nearly 10 mg of samples were weighed into a platinum crucible (5 mm in diameter and 3 mm in height). Simultaneous TG–DTA measurements were performed using ULVAC TGD-9600 at a heating rate of 10 K min^{-1} under flowing N_2 (50 cm^3 min^{-1}). The samples and solid products of the respective thermal events were characterized by means of FT-IR spectroscopy (IR; Shimadzu FTIR 8100), powder X-ray diffractometry (XRD; Rigaku Miniflex) and scanning electron microscopy (SEM; JEOL JSM-T20).

Nearly 5 mg of samples, weighed into an aluminum crucible (4 mm in diameter and 2 mm in height), were subjected to differential scanning calorimetry (DSC). DSC measurements were carried out using an instrument of heat flux type (ULVAC DSC-9400) at various heating rates ϕ under flowing He (30 cm^3 min^{-1}).

3. Results and discussion

3.1. Formation of amorphous calcium carbonate

The samples precipitated from Na_2CO_3–NaOH solutions with pH$\geq$11.2 by adding a $CaCl_2$ solution did not indicate any identifiable diffraction peaks in the XRD. Two distinct patterns of thermal behavior were observed for the samples prepared at pH$\leq$13.0 and pH$\geq$13.5, respectively. Fig. 1 compares the typical TG–DTA curves for the samples prepared at pH 13.0 and 13.5. Both the samples lose their absorbed water molecules until ca. 530 K. The dehydrated products were still amorphous as was shown by means of XRD. A difference was observed in the IR spectra of the dehydrated samples. The absorption band due to the OH stretching at ca. 3000–4000 cm^{-1} was observed only for the dehydration product of the sample prepared at pH$\geq$13.5.

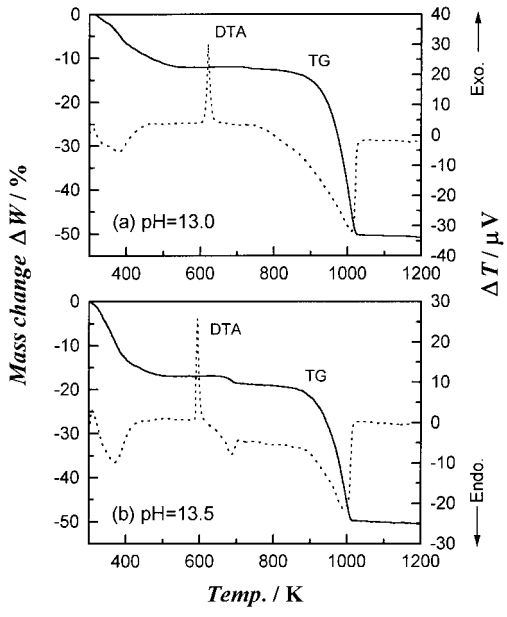

Fig. 1. Typical TG–DTA curves for ACC prepared at pH 13.0 and 13.5.

Following the dehydration, sharp exothermic peaks appeared in the DTA plots for both the samples. Just after the exothermic peak, the sample prepared at pH≤13.0 indicated the XRD pattern and FT–IR spectrum corresponding to those of calcite, whereas a mixed pattern of calcite and $Ca(OH)_2$ was observed for the sample prepared at pH≥13.5.

A subsequent mass-loss of 44.1±0.4% from the crystallization product of the sample prepared at pH≤13.0 was observed, which is in good agreement with the calculated value for the thermal decomposition of calcite to CaO, 44.0%. Two distinct mass-loss processes of the crystallized product were observed for the sample prepared at pH≥13.5. From the XRD pattern and IR spectra of the decomposition products of the respective mass-loss processes, these processes were identified as the thermal decomposition of $Ca(OH)_2$ and $CaCO_3$, respectively. The content of $Ca(OH)_2$ in the crystallization product increased with increasing pH of the mother solution. Accordingly, the amorphous precipitates prepared at pH>13 is called amorphous basic calcium carbonate (ABCC) [2]. The thermal behavior of the amorphous precipitates and their dependence on pH of the mother solution are in good agreement with those reported by Kojima et al. [2].

An interesting finding concerning the dependence of the crystallization temperature of ACC on pH of the mother solution, i.e. a mixed solution of Na_2CO_3–NaOH, reported by Kojima et al. [2] was also reconfirmed in the present study. Fig. 2 shows the dependence of the DTA peak temperature, T_p, of the crystallization exotherm on pH of the mother solution. The crystallization temperature increases with increasing pH, which attains the maximum at ca. 12.7≤pH≤13.0. In the region of pH>13, where the formation of ABCC was observed, T_p decreases with increasing pH.

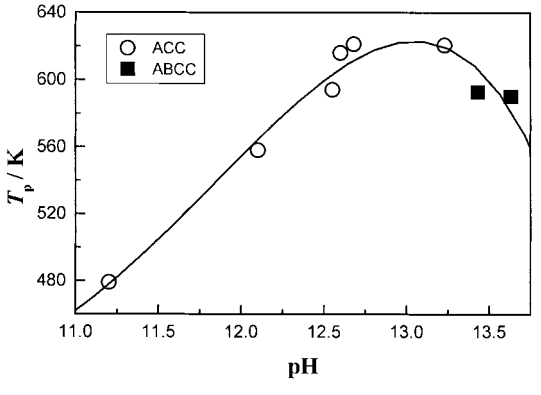

Fig. 2. Dependence of the DTA peak temperature, T_p, for the crystallization of ACC on the pH of the mother solution.

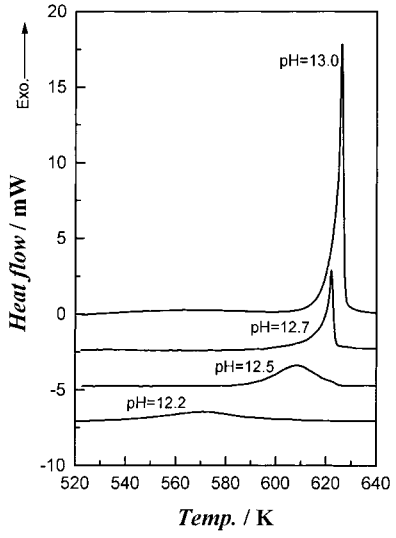

Fig. 3. Typical DSC curves for the crystallization of dehydrated ACC prepared at various pH.

3.2. Crystallization of amorphous calcium carbonate

A series of ACC precipitated in the region 12.2≤pH≤13.0 were subjected to DSC runs. Fig. 3 shows typical DSC curves for the crystallization of dehydrated ACC at a heating rate of 10 K min^{-1}. It is apparent that the change in T_p with pH accompanies the changes in the shape and peak area of the DSC curves. Table 1 lists the enthalpy change ΔH during the crystallization processes. The value of ΔH decreases with decreasing pH, as well as T_p.

From a series of DSC curves for the crystallization of ACC at different heating rates, apparent values of activation energy, E, were determined by the Friedman method [3].

$$\ln\frac{d\alpha}{dt} = -\frac{E}{RT} + \ln\left[Af(\alpha)\right] \quad (1)$$

where α and $f(\alpha)$ are the fractional reaction and the

Table 1
The enthalpy change ΔH and apparent activation energy E for the crystallization of ACC prepared at various pH

pH	Range of ϕ/K min^{-1}	$-\Delta H$/ (kJ (mol $CaCO_3$)$^{-1}$)	E [a]/ (kJ mol^{-1})
13.0	2.0–10.0	12.26±0.22	304.1±23.6
12.7	3.0–15.0	50.7±2.9	261.8±19.9
12.5	3.0–15.0	50.2±2.1	199.9±10.3
12.2	5.0–30.0	39.9±2.1	151.6±13.7

[a] Averaged over $0.2 \leq a \leq 0.8$.

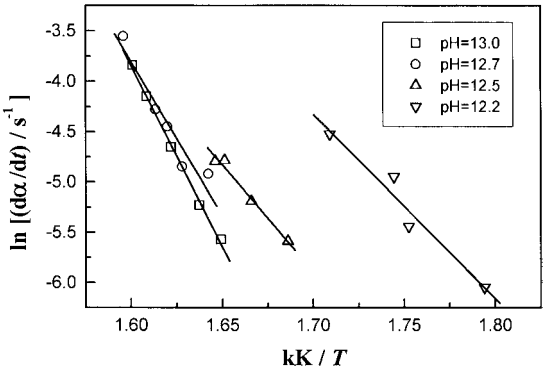

Fig. 4. Typical Friedman plots of ln (dα/dt) against T^{-1} at α=0.5 for the crystallization process of ACC.

kinetic model function in a differential form [4–6], respectively. Other symbols have their standardized meanings. Fig. 4 shows typical Friedman plots of ln (dα/dt) against T^{-1} at α=0.5. Slope of the plot decreases with decreasing pH. The values of E averaged over $0.2 \leq \alpha \leq 0.8$ were also listed in Table 1. The apparent value of E decreases systematically with decreasing pH.

The kinetic dependence on α was reproduced at an infinite temperature by introducing the concept of generalized time θ [7] using the predetermined value of E. The value of θ for a given α can be calculated by the following equation [7–9]:

$$\theta = \frac{E}{\phi R} \frac{\exp(-x)}{x} \pi(x) \quad \text{with} \quad x = \frac{E}{RT} \tag{2}$$

where ϕ and $\pi(x)$ are the heating rate and an approximation function for the exponential integral. In the present study, the $\pi(x)$ function employed is the one proposed by Senum and Yang [10]. θ denotes the reaction time taken to reach a particular α at infinite

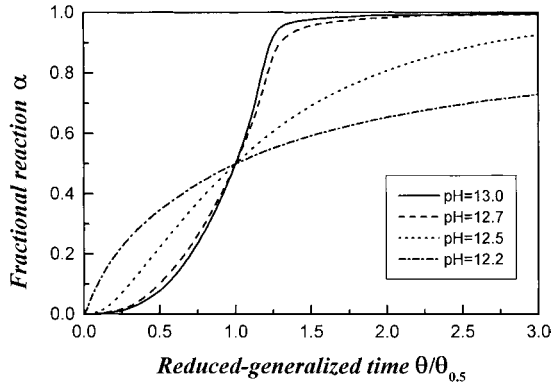

Fig. 5. Experimental master plots at infinite temperature, α against reduced, generalized time $\theta/\theta_{0.5}$, for the crystallization of ACC.

temperature. Fig. 5 shows the dependence of kinetic rate behavior on α at infinite temperature as the plot of α against reduced, generalized time $\theta/\theta_{0.5}$ [11]. The experimental master plot at infinite temperature changes drastically with the pH. An appropriate kinetic model function $g(\alpha)$ was determined through plotting various $g(\alpha)$ against θ, according to the kinetic equation at infinite temperature [7,12,13].

$$g(\alpha) = A\theta \tag{3}$$

where $g(\alpha)$ is the kinetic model function in an integral form [4–6]. Table 2 lists the most appropriate $g(\alpha)$ for the crystallization of ACC, together with the apparent pre-exponential factor A calculated from the slope of the $g(\alpha)$ vs. θ plot. The rate behavior of the crystallization processes can be characterized predominantly by the nucleation and growth model, known as the Johanson–Mehl–Avrami–Erofeev–Kolgomorov (JMAEK) function [4–6]; $g(\alpha)=[1-(1-a)]^{1/m}$. The kinetic exponent of the JMAEK equation decreases

Table 2
Appropriate kinetic model functions $g(\alpha)$ and apparent values of A for the crystallization of ACC prepared at various pH

pH	$g(\alpha)$	m	γ [a]	A [b]/s^{-1}
13.0	$[-\ln(1-\alpha)]^{1/m}$	4	0.9927	$(2.59\pm0.05)\times10^{16}$
12.7	$[-\ln(1-\alpha)]^{1/m}$	4	0.9946	$(3.96\pm0.16)\times10^{16}$
12.5	$[-\ln(1-\alpha)]^{1/m}$	1	0.9997	$(1.96\pm0.29)\times10^{17}$
12.2	$[-\ln(1-\alpha)]^{1/m}$	0.5	0.9990	$(5.43\pm1.30)\times10^{18}$

[a] Correlation coefficient of linear regression analysis of the $g(\alpha)$ vs. θ plot.
[b] Averaged over $0.2 \leq \alpha \leq 0.8$.

with decreasing pH of sample preparation. Because the JMAEK equations are derived on the basis of simplified assumptions on the physics and reaction geometry of the nucleation and growth processes, the complicated specific reaction mechanism cannot always be accommodated satisfactorily by the idealized kinetic models [14–18]. It is expected, however, that the apparent agreement with the JMAEK function and systematic change in the kinetic exponent observed for the present series of crystallization processes suggest, at least qualitatively, the changes in the kinetic characteristics of the crystallization processes. Increase in the concentration of the possible nucleation sites and variation in the rate controlling step due to the change in the temperature region of the crystallization processes are pointed out as probable reasons for the decrease in the kinetic exponent with decreasing pH of the mother solution [19]. While the apparent values of E decrease with decreasing pH, the apparent A values increase with decreasing pH. This behavior is contrary to the well-known kinetic compensation effect [18,20].

Fig. 6 shows typical SEM images of ACC dehydrated at ca. 425 K. ACC is an aggregate of fine spherical particles with the particle size of <0.05 μm. No distinguishing differences could be observed on the SEM images of dehydrated ACC prepared at different pH. Fig. 7 compares typical SEM images of the crystallized samples prepared at pH values of 13.0 and 12.2. The larger particles of calcite are found for the crystallized sample prepared at pH 12.2. The particle size of the crystallization product decreased systematically with increasing pH of sample preparation.

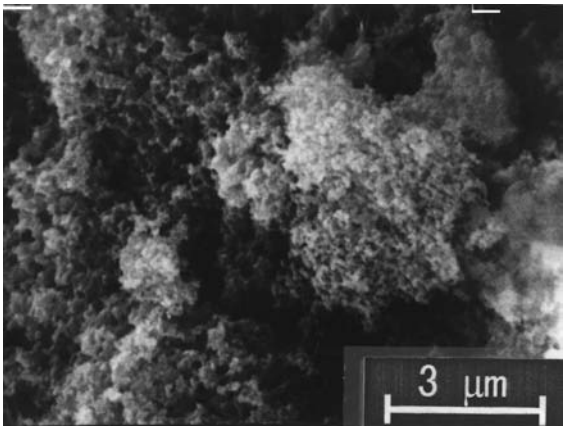

Fig. 6. A typical SEM image of dehydrated ACC prepared at pH 12.7.

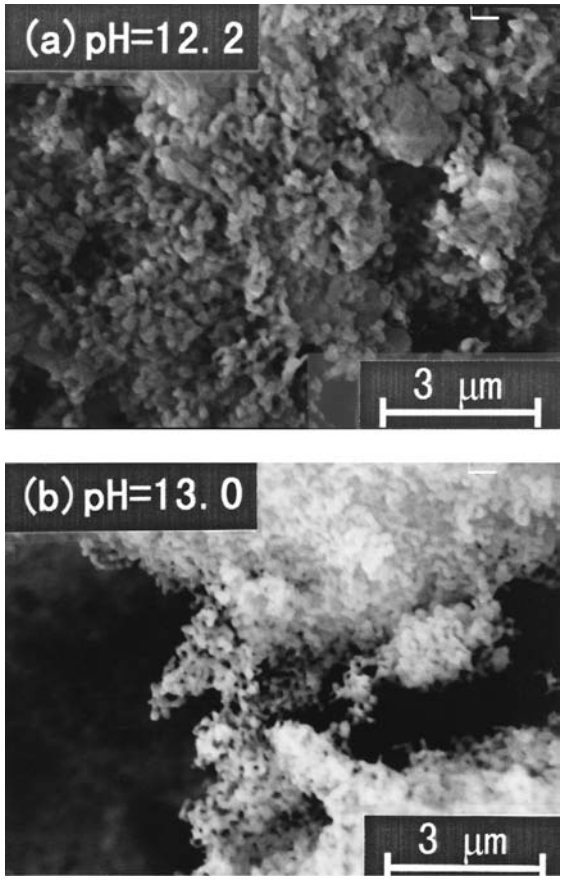

Fig. 7. Typical SEM images of the crystallization product by heating ACC prepared at pH values of 12.2 and 13.0.

From the above results, it is expected that the thermodynamic state of ACC change depends on the pH of preparation. The change of ΔH values for the crystallization process with pH may be explained as one of the results of such changes in the amorphous state. It is apparent that the degree of atomic ordering of ACC increases with decreasing pH, although XRD shows no distinguished diffraction peaks. More sites of possible nucleation are expected for ACC prepared at lower pH, which might result in the observed decreases in the apparent E value and kinetic exponent m in the JMAEK equation with decreasing pH. Accordingly, the crystallization of ACC prepared at pH value in the 12.7–13.0 range,

characterized by the rapid DSC exotherm at the higher temperature region, seems to take place through the consecutive and/or concurrent processes of nucleation and growth. On the other hand, ACC prepared at pH in the 12.2–12.5 range crystallizes by accompanying the moderate exotherm at the lower temperature region, which proceeds probably through the growth of the pre-existing nuclei. Such differences in the crystallization kinetics can be one of the reasons for the change in the particle size of the crystallization products.

4. Conclusion

ACC can be prepared from an aqueous system of $CaCl_2$–Na_2CO_3–NaOH within the $11.2 \leq pH \leq 13.0$ range. On heating, ACC loses the absorbed water until ca. 530 K. With decreasing pH of preparation, the temperature of in-situ crystallization of dehydrated ACC decreases systematically, accompanied by decreases in the ΔH and apparent E for the crystallization. Change in the crystallization processes with decreasing pH can be characterized by the decrease in the kinetic exponent of the JMAEK equation. The particle size of the crystallization products tends to increase with decreasing pH of ACC preparation due to the effects of the different crystallization kinetics.

References

[1] See, for example J. Johanson, H.E. Merwin, E.D. Williamson, Am. J. Sci. 33 (1916) 471; J.E. Gillott, J. Appl. Chem. 17 (1967) 18; L. Brecevic, A.E. Nielsen, J. Cryst. Growth 98 (1989) 504; T. Yasue, A. Yoshiyama, Y. Arai, Phosph. Res. Bull. 1 (1991) 728; T. Yasue, Y. Kojima, H. Inoue, Y. Arai, J. Ceram. Soc. Jpn 98 (1990) 483, in Japanese.
[2] Y. Kojima, A. Kawanobe, T. Yasue, Y. Arai, J. Ceram. Soc. Jpn 101 (1993) 1145, in Japanese.
[3] H.L. Friedman, J. Polym. Sci., Part C 6 (1964) 183.
[4] M.E. Brown, D. Dollimore, A.K. Galwey, Reactions in Solid State, Elsevier, Amsterdam, 1982.
[5] J. Sestak, Thermophysical Properties of Solids, Elsevier, Amsterdam, 1984.
[6] H. Tanaka, N. Koga, A.K. Galwey, J. Chem. Educ. 72 (1995) 251.
[7] T. Ozawa, Bull. Chem. Soc. Jpn 38 (1965) 1881.
[8] J. Malek, Thermochim. Acta 200 (1992) 257.
[9] N. Koga, J. Malek, J. Sestak, H. Tanaka, Netsu Sokutei (Calor. Therm. Anal.) 20 (1993) 210.
[10] G.I. Senum, R.T. Yang, J. Therm. Anal. 11 (1977) 445.
[11] N. Koga, J.M. Criado, J. Am. Ceram. Soc., in press.
[12] N. Koga, H. Tanaka, J. Phys. Chem. 93 (1989) 7793.
[13] N. Koga, Thermochim. Acta 258 (1995) 145.
[14] J. Sestak, J. Therm. Anal. 36 (1990) 337.
[15] N. Koga, H. Tanaka, J. Therm. Anal. 41 (1994) 455.
[16] J. Malek, Thermochim. Acta 267 (1995) 61.
[17] N. Koga, J. Malek, Thermochim. Acta 282/283 (1996) 69.
[18] N. Koga, J. Therm. Anal. 49 (1997) 45.
[19] N. Koga, J. Sestak, Bol. Soc. Esp. Ceram. Vidr. 31 (1992) 185.
[20] N. Koga, Thermochim. Acta 244 (1994) 1.